The Pathophysiologic Basis of Fractionated and Complex Electrograms and the Impact of Recording Techniques on Their Detection and Interpretation

Jacques M.T. de Bakker, PhD; Fred H.M. Wittkampf, PhD

Extracellular electrograms, recorded directly from the heart, are the hallmarks of invasive cardiac electrophysiology and provide information about the electric status of the underlying myocardium. These electrograms are generated by depolarization of cardiomyocytes that generates transmembrane currents in extracellular space and potential differences due to electric resistance of the extracellular medium. In healthy myocardium, the basic configuration of the extracellular electrogram is simple. Under pathological conditions, however, electrograms may consist of multiple components and long duration, which have been attributed to abnormal conduction and arrhythmogenicity. Although complex and fractionated electrograms are presently considered to be a real phenomenon, this was not the case some 20 years ago. Debates about the "fact or artifact" of complex and fractionated electrograms were common.[1] At that time, electrograms consisting of multiple "high frequency" components with low amplitudes and long duration, termed "fractionated," were recorded in patients with healed myocardial infarction during endocardial mapping. Several investigators presumed that fractionated electrograms were artifacts, resulting from movements between electrode and myocardium, filter characteristics of amplifiers, or represented far field effects. A classic example to support the "artifact theory" was the recording of continuous activity from the jello brain.[2] In those days, much attention had been paid to fractionated electrograms in healed myocardial infarction to guide catheter ablation or antiarrhythmic surgery.[3–5] Although artifacts indeed may cause complex electrograms, most of the complex and fractionated electrograms are a "fact" and caused by the peculiar behavior of activation fronts, due to structural and electric complexity of the underlying myocardium. This article delineates the origin of the unipolar extracellular electrogram, reviews the circumstances that cause fractionated and complex electrograms, and discusses the impact of the recording technique on detection and interpretation of multifaceted electrograms.

Origin and Configuration of Unipolar Extracellular Electrograms

Extracellular electrograms arise because of transmembrane currents that occur due to differences in the axial voltage gradient at the interface between activated and inactivated myocardial cells. This is schematically illustrated in Figure 1, which shows a myocardial bundle that is at rest at the right and activated at the left. Activation in the bundle moves from left to right. The action potential causes an axial voltage gradient between activated (+20 mV) and inactivated (−90 mV) sites resulting in axial current flow from the activated toward the inactivated site. Current amplitude is large at the position of the wave front where the voltage gradient is high (site B, 4 arrows). At the left (site A) and the right (site C), the voltage gradient is less steep and the resulting axial current is low (1 arrow). The sum of currents flowing toward a point must be equal to the sum of currents flowing away from that point. This implies that at the back of the activation front (site A), current must flow through the membrane into the cell (3 arrows at the membrane pointing inward), and, in front of the activation front (site C) current flows outward through the membrane (3 arrows at the membrane pointing outward). Thus, the activation front operates as a current dipole, which injects current into extracellular space at the front and retrieves current from extracellular space at the back.[6] Current through extracellular space, which has electric resistance, generates an extracellular voltage difference. The corresponding extracellular potentials, which have been determined by Spach et al[7] for a Purkinje fiber, are illustrated in the upper part of Figure 1. Extracellular potentials are positive in front of the activation front, zero at the activation front, and negative at the back of the activation front. The amplitude of the voltage increases closer to the current dipole. The extracellular potential field moves with the activation front and a recording electrode positioned at a site where the activation front is passing will therefore record an increasing potential when the front is approaching. The potential reaches a maximum when the activation front is very close to the recording site. Then, the potential rapidly decreases to zero and becomes negative with its minimum just as the wave front has past. Thereafter, the negative potential returns to zero as the wave front proceeds. Thus, the extracellular electrogram that is generated by a passing wave front is biphasic, a positive deflection followed by a negative one.

From the Department of Experimental Cardiology, Heart Failure Research Center (J.M.T.d.B.), Amsterdam, The Netherlands; the Departments of Cardiology (F.H.M.W.) and Medical Physiology (J.M.T.d.B.), University Medical Center, Utrecht, The Netherlands; and the Interuniversity Cardiology Institute of the Netherlands (J.M.T.d.B.), Utrecht, The Netherlands.

Correspondence to Jacques M.T. de Bakker, PhD, Academic Medical Center, Department of Experimental Cardiology, Meibergdreef 9, 1105AZ Amsterdam, The Netherlands. E-mail j.m.debakker@amc.uva.nl

(*Circ Arrhythm Electrophysiol*. 2010;3:204-213.)

Circ Arrhythm Electrophysiol is available at http://circep.ahajournals.org DOI: 10.1161/CIRCEP.109.904763

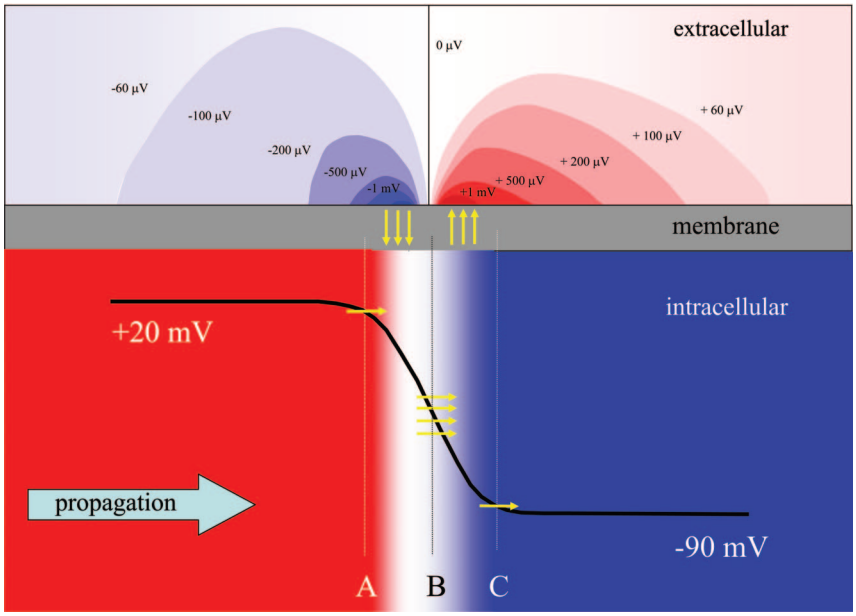

Figure 1. Schematic drawing of the genesis of the extracellular potential field just above the site of activation of a myocardial bundle. The lower part shows potential gradients and axial currents in the intracellular compartment. The upper part reveals the extracellular potential field as generated by the transmembrane current dipole. The extracellular potential field is positive at the front side of the activation front and negative at the back.

This is illustrated in Figure 2, which shows a myocardial bundle that is stimulated electrically at the left. Thus, activation starts at the left and moves to the right. At site B, the wave front is passing and a simple biphasic deflection is generated. At the left, where activation starts, there is no approaching wave front and the local electrogram only has a negative deflection. At the far right, site C, the activation front stops. The recording site just faces the area with positive potentials and consequently the electrogram only has a positive deflection. Thus, in principle, the unipolar electrogram is simple and comprises only a biphasic or monophasic complex.[8] In addition, the configuration of the unipolar electrogram provides information about the activation front at the recording site: (1) an initial negative deflection at the site where activation starts, (2) a biphasic deflection at the site where activation passes, (3) a positive deflection at sites where activation stops, and (4) the downstroke of a unipolar electrogram, the intrinsic deflection, coincides with the upstroke of the action potential of the myocardial cells underneath the electrode.[9,10] This is even the case under ischemic conditions.[9] The initial negative deflection of the unipolar electrogram is helpful in detecting the site of origin of focal activation but may also point to a site of pseudo initial activation such as the exit site of an infarct related ventricular tachycardia (VT). Stevenson and Soejima[11] propose the use of unipolar recordings especially for mapping of focal arrhythmia sources. Haissaguerre et al[12] suggest the use of unipolar recordings to determine accessory pathways, whereas Ito et al[13] recommend the unipolar recording technique for atrioventricular junction ablation, which can be achieved more efficiently and with fewer radiofrequency energy application when guided by unipolar recordings than by bipolar recordings alone.

Bipolar Versus Unipolar Electrograms

A bipolar electrogram is made by subtracting 2 unipolar electrograms recorded at sites that are usually close together (millimeter distance).[2] In the clinical setting, a bipolar recording is often preferred over a unipolar one because the bipolar mode suppresses interference of the electric mains. This is due to the difference in the "field of view" of the unipolar and bipolar electrode. As shown before, an electrode will already pick up a signal generated by the wave front when it is at a distance. This implies that the electrode not only records activity underneath the electrode (the local event) but also at

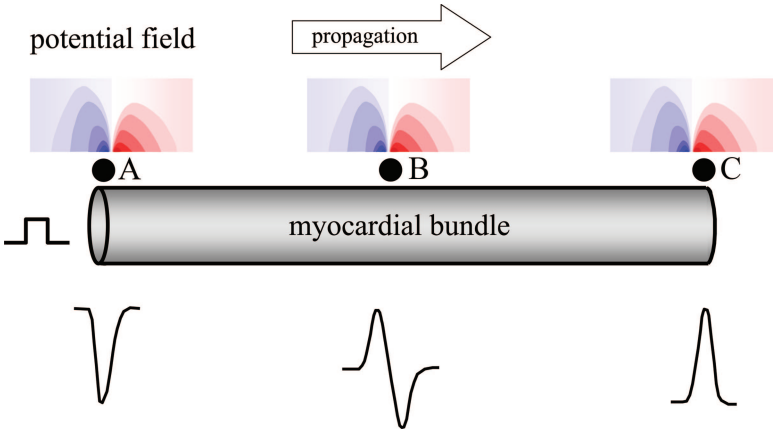

Figure 2. Unipolar extracellular electrograms generated by an activation wave traveling along a myocardial bundle from the left to the right. Color maps show the extracellular potential field generated by an activation front (see also upper part of Figure 1). At the recording site at the left (site A), the activation front starts and the electrogram is negative only because the electrode is only located in the negative part of the potential field. At the recording site in the middle where the activation front is passing (site B), the morphology is biphasic, whereas it is only positive at the right (site C), where activation comes to an end. Here, the recording electrode only meets the positive area of the potential field.

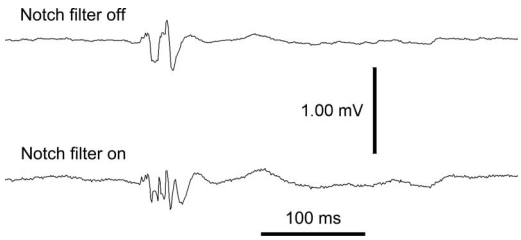

Figure 3. Bipolar recordings made with a mapping catheter (4-mm distal electrode, 1-mm proximal ring electrode, and 2-mm spacing) positioned on the tricuspid valve annulus of a patient with AV nodal reentry tachycardia. Signals were recorded with the Prucka system (30- to 500-Hz bandwidth). The upper tracing shows the signal with the notch filter turned off, the lower tracing with the notch filter turned on. Note the artificial increase in fractionation in case the filter is on.

a distance (remote events). For a current dipole, which represents the activation front, it can be shown mathematically that the amplitude of the signal induced by the wave front attenuates with square of distance for a unipolar and with the third power of distance for a bipolar recording.[14] This means that far-field (remote) signals are more attenuated in the bipolar recording and that the bipolar mode is more sensitive to local effects. Although this is an advantage of the bipolar electrogram, the bipolar recording mode also has several disadvantages. If the poles are close together, the bipolar electrogram approximates the first derivative of the unipolar signal. This means that the bipolar signal is triphasic instead of biphasic if a wave front is passing. The interpretation of bipolar electrograms is therefore more complicated. In addition, the bipolar electrogram is direction dependent; its amplitude depends on the direction of the wave front with respect to the line through the poles of the electrode.

What Makes Electrograms Complex?

Artifacts

As already outlined in the introduction, movement artifacts can cause fractionated electrograms that may complicate signal analysis.[15] In addition, multiple catheters are frequently applied during catheter mapping. Because the catheters are often in close proximity, they may touch each other and cause spiky artifacts. Interference of the mains often overlays the electrogram with a 50/60-Hz signal, frequently accompanied by higher harmonics. In sporadic cases, the interference fluctuates and may give the impression that intervals with fractionation arise in the electrogram. Another type of artifact, not related to the heart is the electromyographic interference. The deflections are real signals generated by the patient's muscle. They often occur in intervals and such fractionation may be misleading, because it is not cardiac in origin.[16] Such artifacts may especially arise when unipolar recordings are applied.

Filtering

To suppress interference from the mains, remote signals such as the ventricular complex in the left atrium, and baseline drift, electrograms are routinely filtered. This allows higher amplification without compromising the quality of the baseline. Filtering, however, may also artificially add deflections

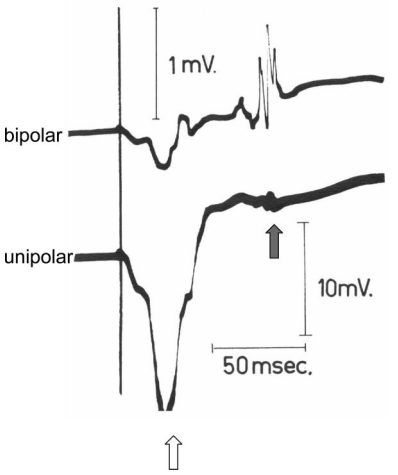

Figure 4. Bipolar (upper tracing) and unipolar (lower tracing) recording made in infracted myocardium. The first component in both tracings is caused by activation in remote healthy myocardium (open arrow), whereas the second component (bold arrow) is the local one, caused by surviving myocardial bundles in the infarcted area. Note that in the unipolar recording the remote component is large and the local component low in amplitude. For the bipolar recording, both components have similar amplitudes; however, deflections of the local component are much sharper.

to the electrogram. In Figure 3, the bipolar electrogram from an ablation catheter with a 4-mm distal electrode and 1-mm proximal ring electrode (2-mm spacing) is bandpass-filtered (30 to 500 Hz), but once with the 50 Hz notch filter off and once with the notch filter on (Prucka System, General Electric). Such filtering clearly adds components to the electrogram that may be interpreted as fractionation and this may become a source of error in finding ablation targets if based on fractionated electrograms.

Remote Activation

Remote signals may affect the local electrogram and a delay between both may lead to an apparently fractionated signal. As shown before, the unipolar recording is more sensitive to remote activity than the bipolar one, but also the latter is not free from deflections caused by remote activations. Typically, deflections are caused by remote ventricular activation that may interfere with local atrial deflections in recordings from the atrium. Depending on the size and configuration of the remote ventricular complex, the atrial deflection may appear as fractionated. However, usually the surface ECG is recorded simultaneously with atrial or ventricular signals, which allows detection of the ventricular component in the atrial recording.[17] More complex and disturbing during atrial recordings may be deflections caused by remote activation in other parts of the atrium, as discussed in the next section.

Infarcted myocardium also is notorious for remote complexes caused by activation in healthy surrounding myocardium.[8] In this case, combined unipolar and bipolar recordings can be very helpful as the unipolar electrogram puts the large remote component in the foreground, whereas the bipolar electrogram enhances the local component (Figure 4).

Adjacent Structures

Many structures in the heart that are activated at different times are anatomically located close to each other. Thus, local

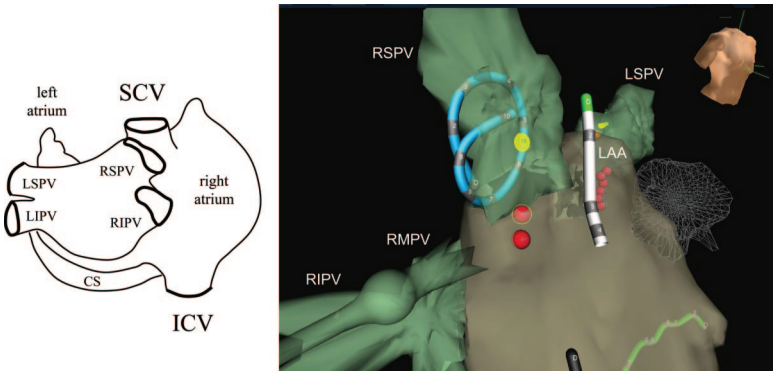

Figure 5. Anatomic reconstruction (NavX system) of the left atrium of a patient with paroxysmal AF showing close proximity of RSPV (circular mapping catheter) and SCV (conventional mapping catheter) is shown at right. Close proximity of the SCV and RSPV is schematically illustrated at the left.

activation recorded at one structure can be disturbed by (remote) activation generated by the other structure. This is important to realize, because it may affect decisions with regard to interventions. For instance, the right superior pulmonary vein (RSPV) is close to the superior caval vein (SCV) (Figure 5, left panel).[18] Similarly, as discussed before, the left superior pulmonary vein and sometimes also the left inferior pulmonary vein are close to the left atrial appendage. Electric isolation of the pulmonary veins (PVs) by means of catheter ablation is a standard procedure to treat AF. Success of isolation is tested by recording activity from the PVs during sinus rhythm or atrial stimulation. If electric isolation is complete, no activity evoked at the atrium will be recorded at the PV. However, activity in adjacent structures might suggest that isolation is incomplete. The right panel of Figure 5 shows a circular mapping catheter in the RSPV and a conventional one in the SCV (in front of the left atrial appendage). Tracings in Figure 6 are obtained with these catheters during sinus rhythm and show that activity in the SCV (MAP 1,2) gives rise to remote deflections in the RSPV. Note that compared with the local RSPV activity (bold arrows) remote SCV deflections in the RSPV (open arrows) occur 2 to 1 and coincide with the SCV deflection, supporting their SCV origin. Such remote deflections in the RSPV (or other PVs) might erroneously be interpreted as failed isolation of the RSPV. During AF, the deflections might be interpreted as highly fractionated RSPV signals.

Anisotropy

Cardiac tissue is anatomically and electrically anisotropic, which is caused by the cell morphology in conjunction with the electric coupling between the cells, mediated by gap

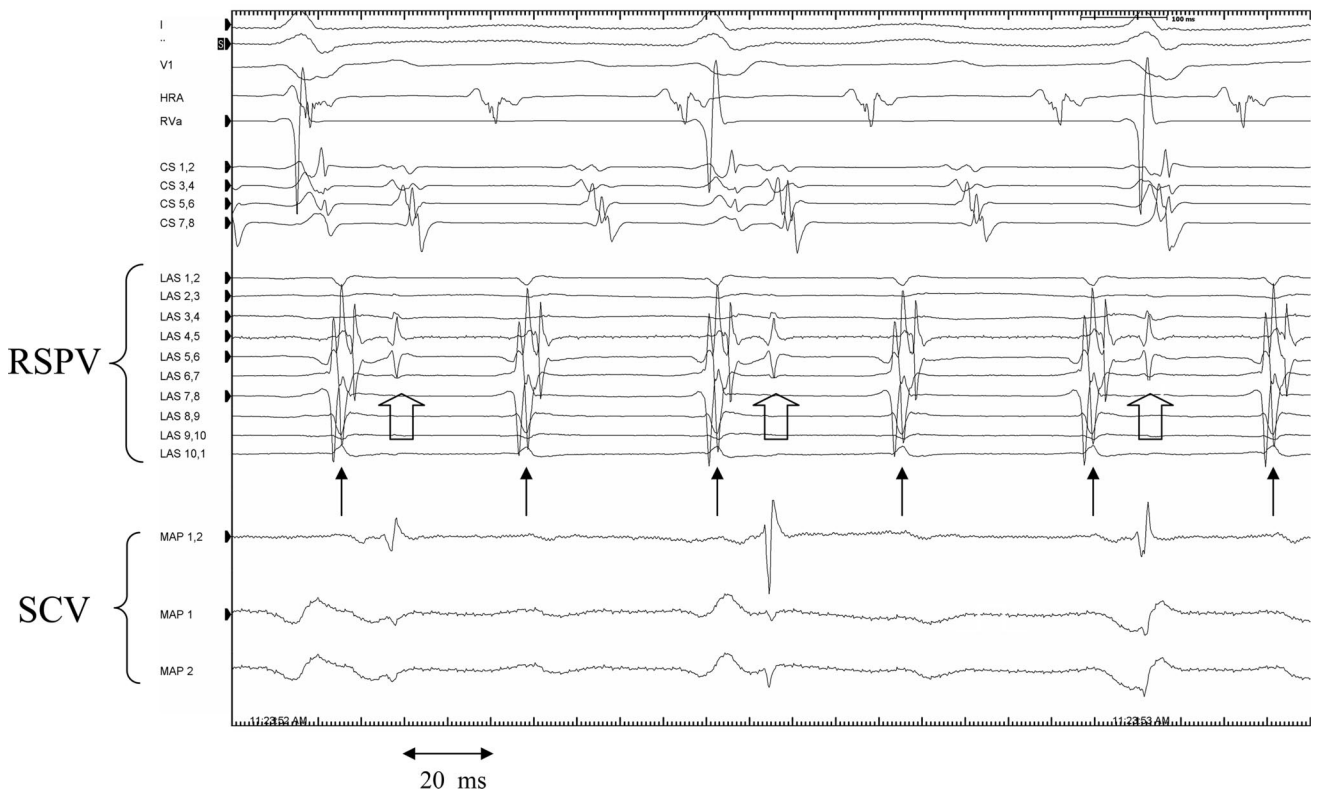

Figure 6. Tracings are surface leads and recordings from the atrium, coronary sinus, RSPV, and SCV made during sinus rhythm in the patient of Figure 5. SCV activity (deflections in map1,2) is detected in the RSPV (open arrow). Bold arrows indicate activity of the RSPV.

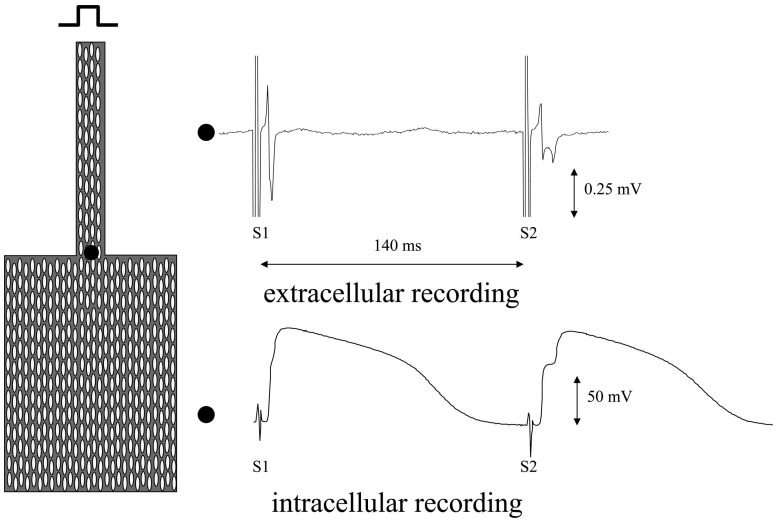

Figure 7. Extracellular and intracellular electrograms recorded at a site where a sudden change in bundle diameter occurs. Recordings were made in a patterned cell culture of neonatal rat cardiomyocytes (schematics at the left). During a basic stimulus S_1, the extracellular complex is biphasic and the upstroke of the action potential almost smooth. After a premature stimulus S_2, the extracellular deflection becomes fractionated and the action potential shows a prominent step in the upstroke. These changes are initiated by the mismatch between current supply and current demand at the discontinuity, which causes conduction delay at the discontinuity.

junction proteins. This results in faster propagation of activation parallel to the fiber direction as compared with propagation perpendicular to the fibers. The configuration of the unipolar extracellular electrograms recorded at sites where the activation front runs parallel to the fiber direction follows the simple rule of the biphasic deflection at the site where activation passes. However, Spach et al[19] have shown that electrograms recorded at sites where activation proceeds perpendicular to the fiber direction deviate from this simple concept and are more complex. At these sites, where activation passes, the associated biphasic deflection is preceded by a small negative one. This deflection arises because of a remote effect of the distant but large wave front that runs parallel to the fibers.[6,19]

Overlaying Structures

In several parts of the heart, myocardial structures that often have different electrophysiological characteristics, overlay. These structures may be totally or partly isolated from each other by collagen and arise in various parts of the heart. An obvious example is presented by the bundle branches and Purkinje fibers, which are isolated from surrounding myocardial tissue by a sheath of collagen. Electric recordings from myocardium near these structures will result in electrograms that reflect both myocardial and Purkinje activity.[20,21] These deflections can often be distinguished, because of differences in their characteristics (sharpness and amplitude). The AV junctional area is much more complex and separation of the different tissue types (atrial cells, transitional cells, and compact nodal cells) is not complete but comprises an intermingling of myocardial cells and fibrosis.[22–24] At the atrial level, the overlaying structure of left atrial myocardium and excitable coronary sinus sleeve is of interest and may result in complex electrograms.[25–27] Myocardial tissue from atrium and coronary sinus are isolated at most sites, but connections may be present at some sites. Therefore, recordings from the inside of the coronary sinus often show multiple deflections because of activation in the 2 different structures.

Alterations in Conduction Velocity

There are several causes for changes in conduction velocity that might affect the complexity of electrograms.

Wave Front Curvature

Electric barriers in the heart, being either anatomically or functionally determined, will force activation fronts to curve around the pivot points.[28,29] At these sites, conduction slowing arises because of source-sink mismatches.[30] As delay arises at the pivot point, the positive deflection caused by the approaching wave front and the negative deflection caused by the receding front are separated, which results in 2 deflections instead of 1 at that location.

Tissue Discontinuities

A sudden change in conduction velocity may arise at tissue discontinuities. If the diameter of a myocardial bundle increases abruptly, current-to-load mismatch may occur at the connection site. The current that the thinner section delivers may not be sufficient to activate the thicker bundle instantaneously. This results in conduction delay and complex electrograms. The delay imposed by current-to-load mismatch is also reflected in the action potential at the discontinuity, which shows a step in the upstroke (Figure 7).[31] Discontinuities in conduction velocity also arise at sites where tissue types with different excitability or coupling characteristics are connected. An extreme example is the interface between myocytes and fibroblasts. Fibroblasts couple electrically to myocardial cells and stretches of fibroblasts in between strands of myocytes are able to propagate the action potential, albeit at a large conduction delay.[32] Impulse transmission along stretches of cardiac fibroblasts as long as 0.6 mm has been observed; conduction delay over this distance was 30 ms, corresponding to a apparent conduction velocity of 0.02 m/s. At present, there are no data available of the role of fibroblasts in situ. Data about conduction in surviving myocardial strands in infarcted myocardium makes it unlikely that fibroblasts play a major role in conduction slowing.[33]

Evidence for fractionated electrograms caused by sudden changes in cell-to-cell coupling is supported by computer modeling. In a model for propagation, Lesh et al[34] showed that fractionated electrograms arose if a uniform wave front encounters a region of increased cellular coupling resistance.

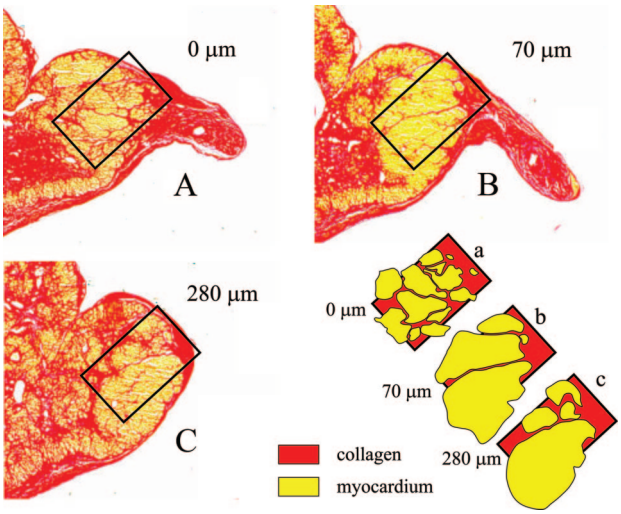

Figure 8. Histological sections of a human papillary muscle stained for collagen with picrosirius red. Sections were taken perpendicular to the long axis of the papillary muscle. Sections are 70 and 210 μm apart. The right lower panel shows the distribution of collagen (red) and myocardium (yellow) for corresponding areas indicated by the squares in the sections. The upper area a shows multiple myocardial bundles separated from each other by collagen. A number of bundles in area a merges in area b of section B but appear to divide again at level C. These data show that the infarcted papillary muscle is characterized by merging and diverging myocardial bundles.

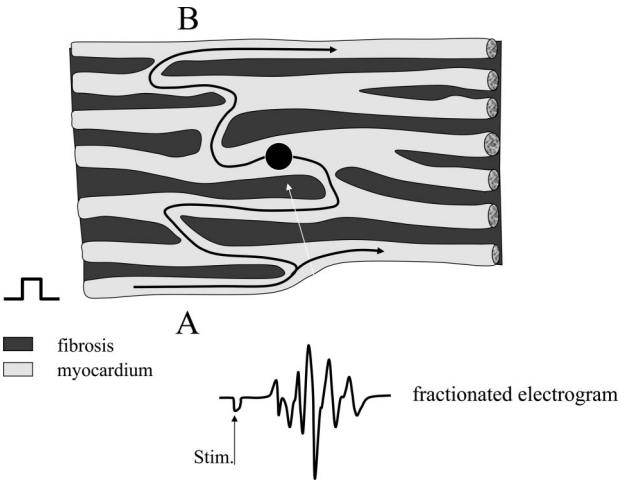

Figure 9. Schematic representation of infarcted myocardium consisting of merging and diverging myocardial bundles. Activation induced by stimulation at site A can reach site B only by following the indicated zig-zag path (arrow). The electrode in the middle will record activation in the various bundles. However, because activation in these bundles is asynchronous, the electrode will record multiple, separated deflections.

Fibrillatory Conduction

Electrograms recorded at sites with structural and/or functional discontinuities may be close to normal during basic stimulation but become complex and fractionated after premature stimulation if sodium current availability is reduced. In the right atrium, the pectinate muscle network is an area with structural complexities where functional conduction block may occur. This was nicely illustrated in isolated, coronary-perfused sheep right atrium by Berenfeld at al.[35] The investigators stimulated the Bachman bundle at different frequencies and recorded the electric activity of the crista terminalis and pectinate muscles optically. Up to a pacing rate of 6.3 Hz, no gross differences in the activation pattern occurred. At frequencies above 6.7 Hz, prominent zones of functional conduction block occurred, which were accompanied by increased complexity of the extracellular electrograms. As observed at tissue discontinuities, action potential upstrokes were complex and revealed multiple upstrokes.

Complex fractionated electrograms have been suggested as target areas for ablating AF.[36] Intraoperative observations showed that these complex electrograms localized at areas of conduction block and pivot points for reentry.[37] Recent studies show that wave front collision, functional conduction block, wave break, and wave fusion all may cause complex and fractionated electrograms in AF.[38,39]

Asynchronous Conduction

In cardiac disease, structural and electric remodeling occur and may be accompanied by remodeling of the autonomic nervous system.[39,40] Structural remodeling may involve changes in cell size, increased collagen deposition, and myocardial fiber disarray. Collagen deposition appears to be a major component in the remodeling process because the majority of cardiac diseases is accompanied by an increase in cardiac fibrosis.[41,42] Although collagen constitutes the framework in which the cardiomyocytes are embedded to give the heart its mechanical rigidity, an increase in the amount of collagen will electrically separate the myocardial cells and prevent the formation of wide, coherent wave fronts. The electrophysiological and anatomic basis for fractionated electrograms recorded in regions where infarct healing caused separation of myocardial fibers was provided by Gardner in 1985.[5] Despite normal transmembrane potentials, activation time was prolonged and inhomogeneous in areas where fractionated electrograms were recorded.

Increased collagen deposition often causes a complex network of intermingled collagen and myocardial fibers.[33] Figure 8 shows the histology of an infarcted human papillary muscle at 3 different levels, 70 μm and 210 μm apart. The schematic drawing at the right shows that separated bundles at level A merge at level B but diverge again at level C. A schematic representation of the merging and diverging bundles is illustrated in Figure 9. When stimulating site A, activation can reach site B only by following the zig-zag route as shown (arrow). The recording electrode in the center of the preparation will not only record activity in the bundle underneath the electrode but also activity of wave fronts propagating in distant bundles. Because of asynchronous activation in the various bundles, multiple deflections will arise, which results in fractionated electrograms.

It is important to realize that a simple, biphasic electrogram could arise if activation proceeds parallel to the fiber orientation in the structure of Figure 9. This is the case if all the bundles at the left are activated at the same time. Indeed, there are still small wave fronts in the various bundles, but, because activation is synchronous now, the deflections they generate at the recording site occur simultaneously, resulting in a single deflection (electric signals at the same recording site

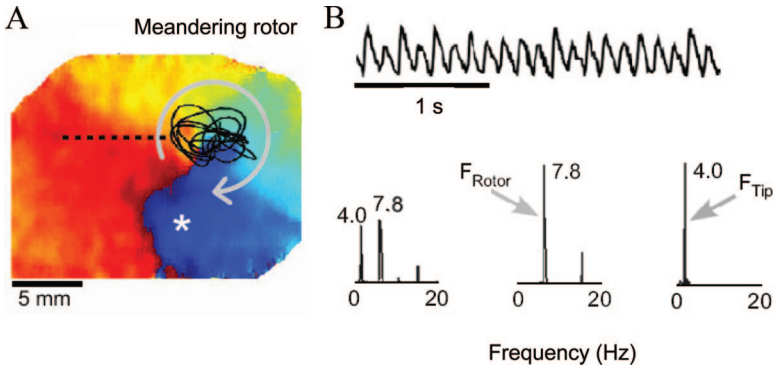

Figure 10. A, Snapshot of reentrant activity in the left atrial free wall (blue, full repolarization; yellow, full depolarization). The clockwise rotor rotates at approximately 7.8 Hz. Time-space trajectory of the tip is shown in black. B, Tracing is the optical signal recorded at the asterisk. Spectra are from the optical signal (left), the periodic constituent (middle, dominant peak at 7.8 Hz), and the residual constituent (right, dominant peak at 4.0 Hz). Periodic constituent reflects periodicity of the rotor (F_{Rotor}), residual constituent indicates the tip meandering component (F_{Tip}). Adapted from Zlochiver et al.[47]

add). Thus, in such structures the direction of a wave front will determine the complexity of the extracellular electrogram. The complexity may increase over time. Gardner et al[5] showed in a canine infarct model a progressive widening of fractionation in the infarct zone with increasing age of the infarct. Similar results in patients with healed myocardial infarction have been reported by Bogun at al.[43]

Structural complexity imposed by branching and joining muscle bundles and sudden changes in fiber orientation as observed in fiber disarray may all give rise to discontinuous conduction, which is associated with multifaceted electrograms.[44]

Role of Conduction Parameters in Fractionated Electrograms

Uniform Versus Nonuniform Conduction Slowing

Although slow conduction has been associated with fractionated electrograms, it depends on the mechanism by which conduction slowing is induced, whether fractionation indeed occurs. As illustrated before in experimental and modeling studies, discontinuous conduction will cause fractionation of the electrogram. In contrast, a homogeneous reduction of the conduction velocity may not result in split electrograms. Jacquemet et al[45] induced slow conduction in a 2D computer model for propagation of the electric impulse in 3 different ways: (1) by a homogeneous reduction of the fast inward sodium current, (2) by a uniform decrease in transverse coupling of myocardial cells, and (3) by introducing a set of collagenous septa disconnecting transverse coupling, as proposed by Spach et al.[46] Septa were aligned with the fiber direction and their length was Poisson distributed. Different microfibrosis densities and lengths of collagenous septa were studied. Results showed that sodium channel blockade up to 80% resulted in conduction slowing. Under these conditions, electrogram amplitude reduced and wave form duration prolonged, but fractionation did not occur. Reduced transverse coupling resulted in conduction slowing as well and had a similar effect on the extracellular potentials, but no fractionation was observed. In contrast, slow conduction induced by microfibrosis resulted in prominent fractionation of the electrograms. Increasing density and length of septa increased the amount of fractionation. This once more emphasizes the role of discontinuous conduction in the generation of fractionated electrograms. With the same model, the authors confirmed that fractionation increases with the size of the electrode and that bipolar recordings revealed a larger number of deflections than the corresponding unipolar electrogram.

Meandering Rotors

The role of meandering rotors in irregularity of electrograms during AF has recently been studied in a 2D computer model with realistic human atrial action potential ion channel characteristics and in isolated sheep heart.[47] The authors hypothesized that during AF there are 2 underlying contributions to the fractionated electric signal, a periodic and a residual constituent (Figure 10). By using singular value decomposition, they were able to distinguish electrogram activity due to rotational activity of the AF rotor from residual components caused by other sources. The residual component is supposed to characterize the role of a reentrant source in irregular and fractionated activity. Application of the technique to the original data of Nademanee et al[47] indeed showed that the recorded complex electrograms could be divided into strictly periodic and residual components. The periodic components probably occurred due to underlying rotor wave activity, whereas residual components were probably related to the meandering of the spiral wave source.

Kalifa et al[48] studied the relation between dominant frequency distribution and wave fractionation and complex, fractionated electrograms in isolated sheep heart during AF. This model of AF showed regular, highly organized activity in the posterior left atrium. Fractionation of activity occurred at the border of the dominant frequency area where most distinct fractionated activity borders the area with most regular activity. Here, electrograms are most fractionated and the authors suggest that these high-frequency fractionated electrograms can be used to localize sources of AF at the posterior left atrium.

Autonomic Nervous System

Although several studies provide evidence for heterogeneous anatomy and areas of functional conduction block as drivers for complex fractionated atrial electrograms, Lin et al[49,50] suggested an autonomic basis for the formation of these atrial electrograms. In a dog model, the investigators showed that by local application of varying concentrations of acetylcholine during AF, the incidence of inducing local complex fractionated electrograms correlated with the concentration of the drug. In addition, injection of acetylcholine into the anterior right ganglionated plexus too resulted in complex fractionated electrograms. The complex electrograms oc-

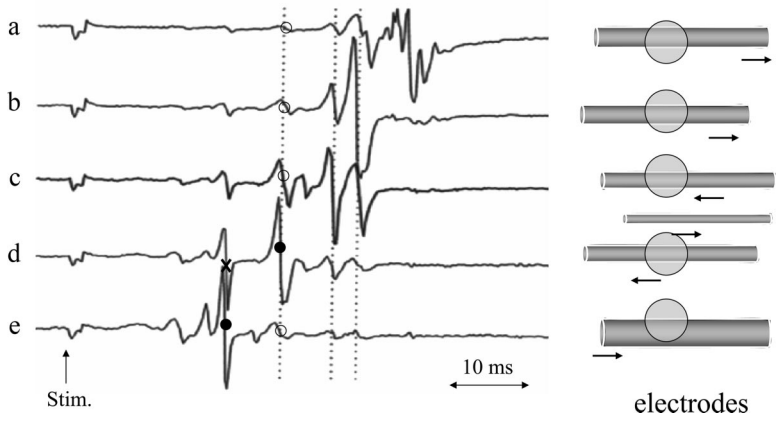

Figure 11. Tracings are unipolar extracellular electrograms recorded at sites along a line perpendicular to a human infarcted papillary muscle. The myocardial bundles that comprise the papillary muscle underneath the recording electrodes are shown at the right. The highly fractionated electrograms are composed of local and remote components. Local components can be distinguished by comparing them with deflections occurring at the same time in neighboring recordings (see text for explanation).

curred distant from the site the drug was injected and were eliminated by ablation. The investigators postulated that the induction of complex fractionated electrograms by local application of acetylcholine excites the autonomic nerve terminals, which resulted in activation of distal ganglionated plexus. These plexus cause fractionation of electrograms by releasing neurotransmitters that modulate atrial wave front stability by causing wave breaks.

Distinguishing Local From Remote Activity

Several techniques have been proposed to distinguish local from remote deflections in complex, fractionated electrograms.[51–55]

The question whether a deflection in a fractionated signal is local or remote is often difficult to answer, especially when recordings are made at only 1 position. Figure 11 shows tracings at 5 recording sites of an infarcted human papillary muscle. Histological investigation showed the presence of multiple, separated, parallel running myocardial bundles, as shown at the right. As outlined before, these bundles may connect at certain sites. Recording sites were 600 μm apart and positioned along a line perpendicular to the fiber direction. By comparing clustered deflections in the recordings, it is evident that the global propagation is from site e to site a. However, the actual trajectory of the activation from e to a is unclear. Presumably, the deflection marked by the black dot in tracing d is the local deflection. The arguments for this are the following: (1) Time-equivalent deflections with lower amplitude are present in the electrograms recorded at the other sites (circles); and (2) the amplitude of these deflections decreases with the distance from d (deflections along the left dotted vertical line).

The deflection in tracing d marked by x is generated by activation in the lower bundle. A time-equivalent deflection has its largest amplitude in tracing e (marked by the black dot in tracing e); the amplitude of the deflection fades away for electrograms recorded further away from site e. Thus, if multiple recordings are available, it is sometimes possible to distinguish local from remote components.

A problem arises if the recording area of the electrode covers multiple bundles. In that case, multiple deflections may be present that are all "local." In the clinical situation, the mapping catheter is also used for ablation and its distal electrode is much larger than the ring electrode. With tissue contact, each electrode records but also more or less averages all signals generated by activation underneath its metal surface. Consequently, electrograms from the larger distal electrode may contain fewer high-frequency components than that from the smaller ring electrode. A bipolar electrogram from such electrode pair, both with good tissue contact, may then predominantly reflect events from the ring electrode, especially when the distal electrode is large (ie, 8 mm). Often, however, the proximal ring electrode is not in contact with myocardium. This (the larger distance to activated tissue), too, reduces the high-frequency components of the local electrogram and in that case it may mainly be the tip electrode that determines the bipolar electrogram morphology. Simultaneous recording of both the bipolar and the corresponding unipolar electrograms eliminates confusion about the origin of the various component of the bipolar electrogram. In addition, it reveals the direction of activation, which may be important in analysis and treatment of the arrhythmia.

Conclusion

The studies illustrated before show that the underlying mechanisms of fractioned and complex electrograms are diverse. They may reflect pure local effects but also may be caused by remote activity at the recording site where deflections caused by the local and distant activity merge. It is important to rule out this possibility if fractionated electrograms are used in the clinical setting as a guide for interventions. Discontinuous conduction and sudden changes in conduction velocity may play a role in structurally remodeled myocardium. They may point to areas with impaired conduction, but the involvement in arrhythmogenicity must be proven if such areas are used as target site for intervention. Homogeneous alterations in cell-to-cell coupling and excitability do not cause fractionation of electrograms, but electric remodeling in cardiac disease is often heterogeneous. In that case, irregular conduction may arise through areas with varying degrees of functional conduction block, resulting into fractionated wave fronts and fractionation of the electrograms. Complex and fractionated electrograms point to areas with abnormal propagation of the electric impulse, and it is conceivable that they are involved in arrhythmogenic processes and be an attractive target for treatment. In AF, fractionated and complex electrograms are currently being used as targets for ablation. Although there are data that suggest that fractionated electrograms might indeed be re-

lated to AF drivers, this outline illustrates that fractionation is a complex process the more so because cardiac disease is accompanied by structural, electric, and autonomic remodeling that all may affect fractionation of electrograms. Also, the role of fractionated electrograms as a guide to ablation of VTs is not yet clear. Weiner et al[56] observed that fractionated electrograms recorded during sinus rhythm were more numerous in the infarct border of patients with episodes of tachycardias and fractionated electrograms had longer duration. Sites with fractionated electrograms were supposed to delineate regions where reentry occurs. Kienzle et al,[4] however, showed that fractionated electrograms were widespread in patients with infarct-related VT but also were found in regions outside the tachycardia origin. Recently, Haqqani et al[57] studied patients with and without sustained monomorphic tachycardia and healed myocardial infarction and showed that patients without VT had fewer fractionated, isolated, and very late potentials than patients with VT.

Thus, although fractionated electrograms refer to abnormal myocardial structure and conduction, a direct relation with tachyarrhythmias remains unclear.

Disclosures

Dr Wittkampf is a consultant of St Jude Medical.

References

1. Josephson ME, Wit AL. Fractionated electrical activity and continuous electrical activity: fact or artifact? *Circulation*. 1984;70:529–532.
2. Gallagher JJ, Kasell JH, Cox JL, Smith WM, Ideker RE, Smith WM. Techniques of intraoperative electrophysiologic mapping. *Am J Cardiol*. 1982;49:221–240.
3. Miller JM, Vassallo JA, Hargrove WC, Josephson ME. Intermittent failure of local conduction during ventricular tachycardia. *Circulation*. 1985;72:1286–1292.
4. Kienzle MG, Miller J, Falcone RA, Harken A, Josephson ME. Intraoperative endocardial mapping during sinus rhythm: relationship to site of origin of ventricular tachycardia. *Circulation*. 1984;70:957–965.
5. Gardner PI, Ursell PC, Fenoglio JJ Jr, Wit AL. Electrophysiologic and anatomic basis for fractionated electrograms recorded from healed myocardial infarcts. *Circulation*. 1985;72:596–611.
6. de Bakker JMT, Hauer RNW, Simmers TA. Activation mapping: Unipolar versus bipolar recording. In: Zipes DP, Jalife J, editors. *Cardiac Electrophysiology: From Cell to Bedside*. 2nd edition. Philadelphia: WB Saunders Company; 1995:1068–1078.
7. Spach MS, Barr RC, Johnson EA, Kootsey JM. Cardiac extracellular potentials: analysis of complex wave forms about the Purkinje networks in dogs. *Circ Res*. 1973;33:465–473.
8. Durrer D, Formijne P, van Dam R, van Lier A, Buller J, Meyler FL. The electrocardiogram in normal and some abnormal conditions; in revived human fetal heart and in acute and chronic coronary occlusion. *Am Heart J*. 1961;61:303–316.
9. Janse MJ. Electrophysiology and electrocardiology of acute myocardial ischemia. *Can J Cardiol.* 1986;(Suppl A):46A–52A.
10. Steinhaus BM. Estimating cardiac transmembrane activation and recovery times from unipolar and bipolar extracellular electrograms: a simulation study. *Circ Res*. 1989;64:449–462.
11. Stevenson WG, Soejima K. Recording techniques for clinical electrophysiology. *J Cardiovasc Electrophysiol.* 2005;16:1017–1022.
12. Haïssaguerre M, Dartigues JF, Warin JF, Le Metayer P, Montserrat P, Salamon R. Electrogram patterns predictive of successful catheter ablation of accessory pathways. Value of unipolar recording mode. *Circulation*. 1991;84:188–202.
13. Ito S, Tada H, Naito S, Kutsumi Y, Miyamori I, Nogami A, Oshima S, Taniguchi K. Randomized comparison of bipolar vs unipolar plus bipolar recordings during atrioventricular junction ablation: importance and efficacy of unipolar recording. *Circ J*. 2007;71:874–879.
14. Durrer D, van der Tweel LH. Spread of activation in the left ventricular wall of the dog. *Am Heart J*. 1953;46:683–691.
15. Lin SL, Wang SP, Kong CW, Chang MS. Artifact simulating ventricular and atrial arrhythmia. *Jpn Heart J*. 1991;32:847–851.
16. Gregg RE, Zhou SH, Lindauer JM, Helfenbein ED, Giuliano KK. What is inside the electrocardiograph? *J Electrocardiol*. 2008;41:8–14.
17. Brouwer J, Nagelkerke D, den Heijer P, Ruiter JH, Mulder H, Begemann MJ, Lie KI. Analysis of atrial sensed far-field ventricular signals: a reassessment. *Pacing Clin Electrophysiol*. 1997;20:916–922.
18. Ho SY, Cabrera JA, Tran VH, Farre J, Anderson RH, Sanchez-Quintana D. Architecture of the pulmonary veins: relevance to radiofrequency ablation. *Heart*. 2001;86:265–270.
19. Spach MS, Miller WT III, Miller-Jones E, Warren RB, Barr RC. Extracellular potentials related to intracellular action potentials during impulse conduction in anisotropic canine cardiac muscle. *Circ Res*. 1979;45:188–204.
20. Lazzara R, Yeh BK, Samet P. Functional anatomy of the canine left bundle branch. *Am J Cardiol*. 1974;33:623–632.
21. Berbari EJ, Lazzara R, El-Sherif N, Scherlag BJ. Extracardiac recordings of His-Purkinje activity during conduction disorders and junctional rhythms. *Circulation*. 1975;51:802–810.
22. McGuire MA, de Bakker JM, Vermeulen JT, Opthof T, Becker AE, Janse MJ. Origin and significance of double potentials near the atrioventricular node: correlation of extracellular potentials, intracellular potentials, and histology. *Circulation*. 1994;89:2351–2360.
23. de Bakker JM, Coronel R, McGuire MA Vermeulen JT, Opthof T, Tasseron S, van Hemel NM, Defauw JJAM. Slow potentials in the atrioventricular junctional area of patients operated on for atrioventricular node tachycardias and in isolated porcine hearts. *J Am Coll Cardiol*. 1994;23:709–715.
24. Jackman WM, Beckman KJ, McClelland JH, Wang X, Friday KJ, Roman CA, Moulton KP, Twidale N, Hazlitt HA, Prior MI. Treatment of supraventricular tachycardia due to atrioventricular nodal reentry, by radiofrequency catheter ablation of slow-pathway conduction. *N Engl J Med*. 1992;327:313–318.
25. Chauvin M, Shah DC, Haissaguerre M, Marcellin L, Brechenmacher C. The anatomic basis of connections between the coronary sinus musculature and the left atrium in humans. *Circulation*. 2000;101:647–652.
26. Antz M, Otomo K, Arruda M, Scherlag BJ, Pitha J, Tondo C, Lazzara R, Jackman WM. Electrical conduction between the right atrium and the left atrium via the musculature of the coronary sinus. *Circulation*. 1998;98:1790–1795.
27. Zheng LR, Chen Y, Lian MJ, Wang LH, Zhu JH, Chen JZ, Tiao QM. Atrial double potential associated with electrical connection between the coronary sinus musculature and the left atrium in a patient with Wolff-Parkinson-White syndrome. *J Electrocardiol*. 2007;40:434–436.
28. Danse PW, Garratt CJ, Mast F, Allessie MA. Preferential depression of conduction around a pivot point in rabbit ventricular myocardium by potassium and flecainide. *J Cardiovasc Electrophysiol*. 2000;11:262–273.
29. Fast VG, Kleber AG. Role of wavefront curvature in propagation of cardiac impulse. *Cardiovasc Res*. 1997;33:258–271.
30. Fast VG, Kleber AG. Cardiac tissue geometry as a determinant of unidirectional conduction block: assessment of microscopic excitation spread by optical mapping in patterned cell cultures and in a computer model. *Cardiovasc Res*. 1995;29:697–707.
31. Derksen R, van Rijen HV, Wilders R, Tasseron S, Hauer RN, Rutten WL, de Bakker JM. Tissue discontinuities affect conduction velocity restitution: a mechanism by which structural barriers may promote wave break. *Circulation*. 2003;108:882–888.
32. Gaudesius G, Miragoli M, Thomas SP, Rohr S. Coupling of cardiac electrical activity over extended distances by fibroblasts of cardiac origin. *Circ Res*. 2003;93:421–428.
33. de Bakker JM, van Capelle FJ, Janse MJ, Tasseron S, Vermeulen JT, de Jonge N, Lahpor JR. Slow conduction in the infarcted human heart: 'zigzag' course of activation. *Circulation*. 1993;88:915–926.
34. Lesh MD, Spear JF, Simson MB. A computer model of the electrogram: what causes fractionation? *J Electrocardiol.* 1988;21(Suppl):S69–S73.
35. Berenfeld O, Zaitsev AV. The muscular network of the sheep right atrium and frequency-dependent breakdown of wave propagation. *Anat Rec A Discov Mol Cell Evol Biol*. 2004;280:1053–1061.
36. Nademanee K, McKenzie J, Kosar E, Schwab M, Sunsaneewitayakul B, Vasavakul T, Khunnawat C, Ngarmukos T. A new approach for catheter ablation of atrial fibrillation: mapping of the electrophysiologic substrate. *J Am Coll Cardiol*. 2004;43:2044–2053.

37. Konings KT, Kirchhof CJ, Smeets JR, Wellens HJ, Penn OC, Allessie MA. High-density mapping of electrically induced atrial fibrillation in humans. *Circulation*. 1994;89:1665–1680.
38. Gerstenfeld EP, Gojraty S, Valles H, Roux J, Lavi N, Michele J. Complex fractionated atrial electrograms are often due to wavefront collision or functional block rather than focal triggers in a canine model of atrial fibrillation [abstract]. *Circulation.* 2009;118:S639.
39. Yamabe H, Morisha K, Tanaka Y, Uemura T, Enomoto K, Ogawa H. Analysis of the mechanism responsible for the genesis of the complex fractionated atrial electrogram during atrial fibrillation using 3D non-contact mapping system [abstract]. *Circulation.* 2008;118:S640.
40. Nattel S, Maguy A, Le BS, Yeh YH. Arrhythmogenic ion-channel remodeling in the heart: heart failure, myocardial infarction, and atrial fibrillation. *Physiol Rev*. 2007;87:425–456.
41. Tanaka M, Fujiwara H, Onodera T, Wu DJ, Hamashima Y, Kawai C. Quantitative analysis of myocardial fibrosis in normals, hypertensive hearts, and hypertrophic cardiomyopathy. *Br Heart J*. 1986;55:575–581.
42. Kostin S, Klein G, Szalay Z, Hein S, Bauer EP, Schaper J. Structural correlate of atrial fibrillation in human patients. *Cardiovasc Res*. 2002; 54:361–379.
43. Bogun F, Krishnan S, Siddiqui M, Good E, Marine JE, Schuger C, Oral H, Chugh A, Pelosi F, Morady F. Electrogram characteristics in postinfarction ventricular tachycardia: effect of infarct age. *J Am Coll Cardiol*. 2005;46:667–674.
44. Spach MS, Miller WT III, Dolber PC, Kootsey JM, Sommer JR, Mosher CE Jr. The functional role of structural complexities in the propagation of depolarization in the atrium of the dog: cardiac conduction disturbances due to discontinuities of effective axial resistivity. *Circ Res*. 1982;50: 175–191.
45. Jacquemet V, Henriquez CS. Genesis of complex fractionated atrial electrograms in zones of slow conduction: a computer model of microfibrosis. *Heart Rhythm*. 2009;6:803–810.
46. Spach MS, Heidlage JF, Dolber PC, Barr RC. Mechanism of origin of conduction disturbances in aging human atrial bundles: experimental and model study. *Heart Rhythm*. 2007;4:175–185.
47. Zlochiver S, Yamazaki M, Kalifa J, Berenfeld O. Rotor meandering contributes to irregularity in electrograms during atrial fibrillation. *Heart Rhythm*. 2008;5:846–854.
48. Kalifa J, Tanaka K, Zaitsev, Warren M, Vaidyanathan R, Auerbach D, Pandit S, Vikstrom KL, Ploutz-Snyder R, Talkachou A, Atienza F, Guiraudon G, Jalife J, Berenfeld O. Mechanisms of wave fractionation at boundaries of high-frequency excitation in the posterior left atrium of the isolated sheep heart during atrial fibrillation. *Circulation*. 2006;113: 626–633.
49. Lin J, Scherlag BJ, Zhou J, Lu Z, Patterson E, Jackman WM, Lazzara R, Po SS. Autonomic mechanism to explain complex fractionated atrial electrograms (CFAE). *J Cardiovasc Electrophysiol*. 2007;18:1197–1205.
50. Lu Z, Scherlag BJ, Lin J, Niu G, Ghias M, Jackman WM, Lazzara R, Jiang H, Po SS. Autonomic mechanism for complex fractionated atrial electrograms: evidence by fast Fourier transform analysis. *J Cardiovasc Electrophysiol*. 2008;19:835–842.
51. Anderson KP, Walker R, Ershler PR, Fuller M, Dustman T, Menlove R, Karwandee SV, Lux RL. Determination of local myocardial electrical activation for activation sequence mapping: a statistical approach. *Circ Res*. 1991;69:898–917.
52. Anderson KP, Walker R, Fuller M, Dustman T, Ershler PR, Lux RL. Criteria for local myocardial electrical activation: effects of electrogram characteristics. *IEEE Trans Biomed Eng*. 1993;40:169–181.
53. Cabo C, Wharton JM, Wolf PD, Ideker RE, Smith WM. Activation in unipolar cardiac electrograms: a frequency analysis. *IEEE Trans Biomed Eng*. 1990;37:500–508.
54. Damiano RJ Jr, Blanchard SM, Asano T, Cox JL, Lowe JE. Effects of distant potentials on unipolar electrograms in an animal model utilizing the right ventricular isolation procedure. *J Am Coll Cardiol*. 1988;11: 1100–1109.
55. Ellis WS, Eisenberg SJ, Auslander DM, Dae MW, Zakhor A, Lesh MD. Deconvolution: a novel signal processing approach for determining activation time from fractionated electrograms and detecting infarcted tissue. *Circulation*. 1996;94:2633–2640.
56. Weiner I, Mindich B, Pitchon R. Determinants of ventricular tachycardia in patients with ventricular aneurysms: results of intraoperative epicardial and endocardial mapping. *Circulation.* 1982:65;856–861.
57. Haqqani HM, Kalman JM, Roberts-Thomson KC, Balasubramaniam RN, Rosso R, Snowdon RL, Sparks PB, Vohra JK, Morton JB. Fundamental differences in electrophysiologic and electroanatomic substrate between ischemic cardiomyopathy patients with and without clinical ventricular tachycardia. *J Am Coll Cardiol*. 2009;54:166–173.

KEY WORDS: ablation ■ arrhythmia ■ electrophysiology ■ heart diseases ■ collagen